Preparation and Characterization of Microcapsules Encapsulating Octyl Methoxycinnamate by Complex Coacervation

X.-L. ZHAO, D. WANG, X.-F. GONG, S.-P. SUN AND Q. LI*

School of Chemistry and Materials Science, Heilongjiang University, [1]Key Laboratory of Chemical Engineering Process and Technology for High-efficiency Conversion, College of Heilongjiang Province, Harbin 150 080, PR China

The aim of this study was to entrap the lipophilic ultraviolet absorber, octyl methoxycinnamate in microcapsuels to enhance its application. A complex coacervation method was established**.** Through the appearance of encapsulated glass beads prepared with different wall materials, gelatin and sodium polyphosphate were selected as wall materials because of dense structure and less adhesion. The effects of three variables, core/(core+wall) ratio, pH at complex coacervation, and amount of cross-linking agent, on encapsulation efficiency were studied. Response surface methodology was employed to optimize the technology, and a polynomial regression model equation was generated. The optimization method enabled to predict the response variable value within the experimental range with good agreement between the predicted and experimental values. The microcapsules under the optimized conditions appeared spherical in shape with smooth nonporous surface and no tendency to aggregation. The photodegradation percentage of octyl methoxycinnamate after exposing to ultraviolet irradiation was determined and the transdermal permeation pattern of octyl methoxycinnamate and its photodegradation product from various formulations was estimated *in vitro***.** From the results obtained, the microcapsules had achieved decreasing transdermal permeation of octyl methoxycinnamate and its photodegradation product, enhancing the accumulation of the sunscreen at the administration site, and then increasing the protection effect and safety. This study revealed the potential of sunscreen microcapsules as new skin drug delivery systems.

Key words: Complex coacervation, octyl methoxycinnamate, response surface methodology, transdermal permeation, photodegradation

Ultraviolet (UV) irradiation of sunlight plays the most important role in causing sunburn, photoaging, photosensitization[1,2], and chronic skin disease, such as idiopathic photodermatosis, formation of melanin, inflammatory responses, adverse reactions to the skin immune system, and even skin cancer[3]. Accordingly, the increased awareness of protection against UV radiation damage had fuelled a rise in the use of topically applied sunscreen agents. Health agencies world-wide also advocated the use of sunscreens as a means of lowering the risk of developing skin cancer. The most common active ingredients in these preparations are organic chemical blockers which absorb UV light[4], while the inorganic materials that reflect UV light, such as titanium dioxide and zinc oxide, are oily relatively and block the pores against excreting of sweat and breathing of skin[5,6].

Currently, octyl methoxycinnamate (OMC) represented the most common sunscreen agent in commercially available cosmetics, because it had excellent UV absorption curve and good oil solubility[7]. When this organic UV filters coated on skin superficial areas, the large accumulation within the deeper layers of skin should be considered due to high lipophilicity and strong permeability[8]. Furthermore, the dosage of OMC was increased sometimes to meet a high sunscreen protection factor (SPF) goal. The increased use of OMC aggravated the potential risk[7,9]. It was reported that OMC inhibited the deiodinase activity[10], induced morphological changes in the testes and ovaries of rats[11], and affected secretion of estrogen, reproductive development and nervous system of rat offspring[12-14]. In the United States, European Union, and Australia, it was stipulated that the maximum dosage of OMC was 7.5-10%[15].

There is an increased requirement of innovative technology designed to achieve the higher protective effect and reduce the toxicological risk from the percutaneous absorption. In recent years, microencapsulation technology has exhibited rapid development and been widely applied in pharmaceutical, food, agricultural pesticide, cosmetic, textile, and other related fields[16,17]. It was considered as a promising technology to encapsulate OMC for overcoming the transepidermal penetration and promoting UV absorption ability. Complex

***Address for correspondence**
E-mail: ZHXL100@126.com

coacervation, caused by electrostatic attraction of two oppositely charged colloids, has been used widely to microencapsulate drug components[18,19]. The coating materials can be prepared from gums, polymer electrolyte, polysaccharides, proteins, and lipids[20,21].

In this study, it was attempted to prepare OMC microcapsules by complex coacervation to improve the topical application of OMC. To determine the optimal conditions for microencapsulation, response surface methodology (RSM) was applied. In addition to analyzing the effects of independent variables, this experimental methodology generated a mathematical model to describe fully the microencapsulation process[22,23]. The photodegradation percentage of OMC after exposing to UV irradiation and the transdermal permeation pattern of OMC and its photodegradation product from various formulations was investigated *in vitro*.

MATERIALS AND METHODS

Octyl methoxycinnamate (OMC) was supplied by Hubei Yuancheng Co., Ltd. Gelatin from porcine skin, type B, Bloom 260, was obtained from Xiamen Huaxuan Gelatin Co., Ltd. Arabic gum was obtained from Hunana Mingrui Co., Ltd. Chitosan, low viscosity (22 cps), 200,000 Daltons molecular weight, 88.1% deacetylation, was purchased from Shandong AK Biotech Ltd. Sodium polyphosphate was from Tianjin Fengchuan Co., Ltd. Glutaraldehyde (50%), as a crosslinker, was provided by Kermel Co., Ltd. The other chemicals and solvents used in this work were of analytical grade, purchased from Sigma-Aldrich Co., Ltd. Deionised water (electrical conductivity <2 μS cm^{-1}) was used throughout all the experiments.

Selection of wall materials:

In order to screen wall materials, glass beads, an insoluble solid, were used as core materials. As the surface condition of core materials is very sensitive in microencapsulation[24], glass beads were used after they were immersed in concentrated sulfuric acid for 4 days and washed well by water. The dried glass beads (0.05 kg) were immersed in 300 ml n-hexane, adding an adequate amount of dimethyldichlorosilane, then stirred for 2 h. After stirring, supernatant liquid was removed. The remains were mixed with an adequate amount of n-hexane and stirred again for 30 min to stop the reaction. The above operation was repeated 3 times. The glass beads were dried well and used as cores in microencapsulation.

A complex coacervation method was used. Gelatin was chosen as one of wall materials. Chitosan (polysaccharides), arabic gum (colloids), and sodium polyphosphate (polymer electrolyte) was chose as the other of wall materials, respectively. The details were showed in fig. 1. Scanning electron microscopy (SEM) was used to evaluate the morphology of glass beads microcapsules.

Preparation of OMC microcapsules:

The OMC microcapsules were prepared by the complex coacervation method with gelatin and sodium polyphosphate as wall materials. Gelatin solution (10%, w/w) was obtained by swelling gelatin in deionised water and heating up to 40º until the appearance of a homogeneous solution. Sodium polyphosphate solution (5%, w/w) was dissolved in deionised water. The weight ratio of gelatin to sodium polyphosphate was 10/1. O/W emulsion was prepared by adding OMC [core/(wall+core) ratio: 30-70%] into the gelatin solution at high shear rate of 10 000 rpm (Fluko Homogenizers, model FA25, USA), and then diluted 3-4 times with deionised water (50º). The sodium polyphosphate solution was added slowly to the resulted emulsion. The pH of mixture was adjusted to 4.15-4.55 with 10% phosphoric acid. This mixture was stirred for 30 min. The whole coacervation process was carried out at 50º. The formed primary microcapsules were cooled to 5º in water-ice bath for further precipitation. After adding a certain amount of cross-linking agent, 5% glutaraldehyde (1-4 mM glutaraldehyde/1 g gelatin), the cooling preparation was heated and maintained at 60º, and then stirred for 1 h. The OMC microcapsules were obtained by spray-drying process using a Buchi B-290 mini spray dryer (Switzerland) at an inlet air temperature of 180º, a rotameter setting of 25 mm (300 l/h) for the atomizing air flow, and a pump rate for liquid of 1.5 ml/min. These settings resulted in an outlet temperature of ~120º.

Experimental designs for optimizing the process of microencapsulation:

RSM was established to determine the variation of assessment index with respect to operating parameters, using a three-factor-three-level full factorial design. The core/(wall+core) ratio (X_1, %), pH at complex coacervation (X_2), and glutaraldehyde amount (X_3, mM/1 g gelatin) were selected as the independent variables analyzed. The dependent variable investigated was encapsulation efficiency (EE). The actual variable was coded to facilitate multiple regression analysis (Table 1). The least square regression model was fitted into the responses taken from the experimental data and to define an optimization process of the entrapment percentage.

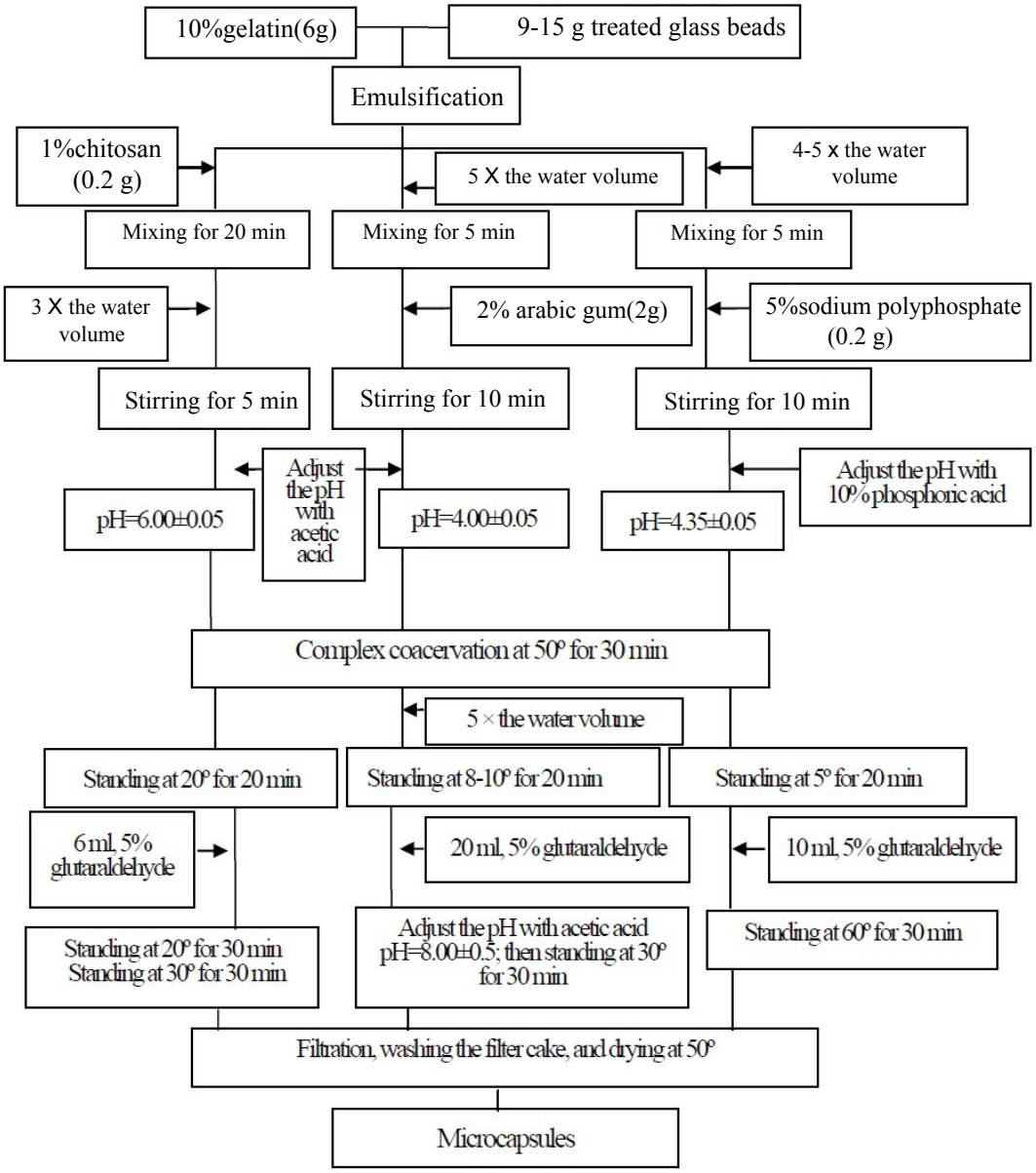

Fig. 1: The process of glass beads microcapsules with different wall materials.

The regression model equation for the EE of OMC that was then evaluated using the quadratic models of the form Eqn. (1) was generated for each response parameter. $Y=\beta_0+\sum\beta_i X_i+\sum\beta_{ii}X_i^2+\sum\beta_{ij}X_iX_j\ldots(1)$, where Y is response calculated by the model, β_0 is a constant, and β_i, β_{ii}, β_{ij} are regression coefficients for intercept, linear, squared and interaction coefficients, respectively; X_i and X_j stand for coded independent variables, the main effects; X_iX_j is the interaction between the main effects. The significant terms in the model were found by analysis of variance for the response. Experimental data were compared with the fitted values predicted by the models in order to verify the adequacy of the regression models.

High performance liquid chromatography (HPLC):

HPLC (Shimadzu, Japan) method was established for the determination of OMC. The system comprised a Model LC-10AT$_{VP}$ pump, a Model 7725i injection valve with a 20 µl sample loop and a Model SPD-10A$_{VP}$ variable wavelength UV/Vis detector set at 310 nm. A C_8 column (250 mm×4.6 mm, 5 µm, Dikma Technologies, China) was utilized and the mobile phase, filtered through a 0.22 µm filter prior to use, consisted of acetonitrile and water (95:5, v/v) at a flow rate of 0.80 ml/min. Chromatography was performed at room temperature. Quantification was carried out by integration of the peak areas using the external standardization method. The respective peak areas were recorded and plotted.

Determination of EE:

The microcapsules were weighed accurately and dispersed in an organic solvent (methanol or acetonitrile) with a known volume. The sample was

TABLE 1: CODED LEVELS OF THE INDEPENDENT VARIABLES USED IN THE EXPERIMENTAL DESIGN

Variables (Units)	Coded, X_i	Coded Levels		
		-1	0	1
core/(wall+core) ratio (%)	X_1	30	50	70
pH at complex coacervation	X_2	4.15	4.35	4.55
glutaraldehyde amount (mM/1 g gelatin)	X_3	1	2.5	4

allowed to stand overnight and away from sunlight. It was filtered through 0.22 μm membrane and the OMC in the resultant filtrate was assayed by HPLC method as described above. Based on the resulting value, the entrapped amount of OMC in the microcapsules was calculated. Each experiment was carried out in triplicate.

The EE of the microcapsules was calculated using the formula: EE (%)=$C_a/C_i \times 100$, where C_a is the calculated drug content in the microcapsules, C_i is the theoretical drug content added initially during the batch preparation.

Scanning Electron Microscopy:

The outer structures of the samples were investigated by scanning electron microscopy (SEM). Dried products were mounted on aluminum stubs and coated with gold (20 nm thickness) using an ion coater (Eiko Engi-neering, model IB-2, Japan). Accelerating voltages of 5 kV was used to observe the morphology of the gold coated specimens. Encapsulated samples were determined by image processing software (Image J, NIST) and captured by automatic image-capturing software.

Particle size analysis:

Mean particle size distribution was measured by Laser particle size scanners (Shimadzu, model SALD-301V, Japan). The size range of the SALD-301V version is 0.1-350 μm. The microcapsules specimens were suspended in dispersion medium, namely water in this experiment, and subsequently analyzed. The results were expressed by volume fraction.

UV absorption experiment:

The UV irradiation was undertaken in a black-box UV analyzer (Gucun, model ZF-20D, China). The different preparations included the free OMC, OMC adsorbed by silicon dioxide (SiO_2), the OMC microcapsules, and OMC microcapsules well-dispersed by addition of SiO_2 were exposed to UV irradiation. The specimens were placed in front of the exit port of the simulator and air cooled during irradiation. After the appropriate interval, the experiment products with a accurate quality were collected and removed into a 10 ml volumetric flask, diluted with acetonitrile and filtered (0.22 μm membrane filter). The resulting solution was evaluated by HPLC, and the degradation percentage of OMC was calculated.

Preparation of four sunscreen creams:

The methanol solution of OMC was directly exposed to UV irradiation for 4-6 days in a black-box UV analyzer, until it became deep yellow. The mixture was then concentrated by rotary evaporation at 40º, and the photodegradation product was obtained[25]. The manufacture process of microcapsules containing photodegradation product was the same as that of OMC microcapsules.

The composition of sunscreen creams was provided as follows: OMC (free or microcapsules), or photodegradation product (free or microcapsules), 14 g (corresponding to free OMC); glyceryl monostearate, 10 g; stearic acid, 26 g; lanolin, 10 g; isopropyl palmitate, 4 g; triethanolamine, 2 g; sorbitol, 2 g; distilled water, 132 g. These ingredients were heated up to 95º until homogeneous emulsion formed. The system was then cooled to the room temperature. The whole preparation was agitated with stirrer at rate of 400-500 rpm.

Transdermal permeation experiment:

Porcine ear skins were used as the *in vitro* model for this study, because its essential permeation characteristics were similar with human skin[26,27]. The percutaneous absorption experiment of the four creams was performed through a drug transdermal diffusion absorption apparatus (Huanghai, model RYJ-6A, China). The treated and dried skin was rehydrated by immersing in the phosphate buffer (pH 7.4) overnight at 5-10º. The skin specimens were mounted on a diffusion cells, and the exposed skin surface area was 3.14 cm^2. The receptor fluid was consisted of the phosphate buffer (pH 7.4) and tween-80 (5%, v/v), and the volume was 6 ml. The solubility of OMC in the medium was checked prior to beginning the analysis. Furthermore, the whole experiment was performed under a constant magnetic stirring speed of 500 rpm at 32º.

The sunscreen cream containing OMC (free or microcapsules) or photodegradation product (free or microcapsules) was applied at a final dose of 1 mg/cm^2 with a uniform spread covered the entire surface over the whole skin area in a thin layer. At predetermined intervals, the receptor fluid of 200 μl were withdrawn and replaced with fresh solution

through the lateral inlet. The samples were filtered through a 0.22 μm membrane filter and analyzed by HPLC, respectively. The photodegradation product was determined by the same HPLC method as OMC, with exception of the detective wavelength of 280 nm.

The experiment was carried out in triplicate. The amount of percutaneous absorption was plotted *vs.* time. The extent of transepidermal penetration of the photodecomposition compounds was evaluated by comparing the peak areas of the analysis specimens.

RESULTS AND DISCUSSION

In general encapsulation process, core material is usually oil drop for the emulsifying process and then covered by wall material in the succeeding stage to complete the microcapsules[18,28]. However, it is remarkably difficult to observe the structure and thickness of coating ingredient. To solve this problem, glass beads with a narrow size distribution, which were prepared by classification of 200 mesh, were used as core material because of their spherical shape and easy treatment to obtain a hydrophobic surface. The surface treatment for glass beads has significant effect on the formation of coating on the beads. Even more fundamentally, the surface treatment will affect how much water the glass takes up from both ambient humidity and the aqueous bath, which could affect the surface of the glass bead[29].

The selection of gelatin was attributed to its biodegradability, biocompatibility, high hydrophilicity and particular gelling property. Most importantly, it exhibited excellent emulsibility compared to the other polymers which needed the participation of emulsifier[30]. The surface morphology of microcapsules covered with different wall materials was presented in fig. 2. As showed in figs, all of three kinds of microcapsules had obvious wrinkle on the surface, and showed smooth appearance (figs. 2b, 2f, and 2j). The apparent shell materials were separated from the glass beads after appropriate grinding (figs. 2c, 2g, and 2k), and the coating exhibited dense structure at high magnification (figs. 2d, 2h, and 2l). Nevertheless, it is a significant aspect that the sunscreen agent can be easy to incorporate in any kind of formulation, which can improve the substantivity of cosmetics towards skin. This requires small diameter and good dispersity with minimum tendency to aggregation. Based on the SEM pictures of three kinds of microcapsules (figs. 2a, 2e, and 2i), it could be concluded that the gelatin-sodium polyphosphate microcapsules had the better dispersity, while the other two showed larger tendency to aggregation. Sodium polyphosphate as one of wall materials had more favorable performance compared to chitosan and arabic gum, and it could be explained that sodium polyphosphate has high solubility, and low molecular weight and viscosity.

Based on the RSM design, EE showed good fitting to the quadratic model (r^2=0.9782). The Model F-value of 70.90 implied that this model was significant. There was only a 0.01% chance that this large "Model F-Value" could occur due to noise. The "Lack of Fit F-value" of 7.57 implied that the Lack of Fit was not significant relative to the pure error. There was a 11.89% chance that this large "Lack of Fit F-value" could occur due to noise. Non-significant lack of fit was good. The regression model equation is, *EE* (%) = $92.60+3.77X_1-2.16X_2+2.72X_3+1.32X_1X_2-2.62X_1^2-2.95X_2^2-2.84X_3^2$.

The coefficients of X_1, X_2, and X_3 in the fitting equation indicated that the EE of microcapsules was significantly influenced by all three variables. As the core/(core+wall) ratio increased, EE increased significantly (positive coefficient of X_1). A possible explanation for this was that only a fixed amount of OMC was probably lost to the external phase during the formation of microcapsules and this loss obviously had a more detrimental effect on EE with relatively lower drug content[28]. After reaching a maximum level, EE started to decline slightly as the core/wall ratio was further increased. This was indicated by the negative coefficient of the square term of X_1 and could be attributed to the practical limitation to the amount of drug that can be incorporated in the microcapsules[31,32]. Furthermore, the microcapsules prepared under the condition of high core/(core+wall) ratio had an extremely thin wall and fragile tridimensional network structure, which would lead to adverse effect on the inhibition of percutaneous penetration. A narrow range of pH (4.15-4.55) for complex coacervation were selected in this experimental design. In this range, EE increased as pH was decreased (negative coefficient of X_2). This could be attributed to the higher degree of complex coacervation reaction between gelatin and sodium polyphosphate at lower pH. In this study, low concentration of glutaraldehyde (5%) was used, because high concentration of crosslinker in the solution existed in the form of polymer which would decrease the crosslinking efficiency and then increase the dosage of glutraldehyde. Within the experimental range, EE increased as the amount of glutaraldehyde was increased (positive coefficient of X_3). The only statistically significant interaction in the EE equation

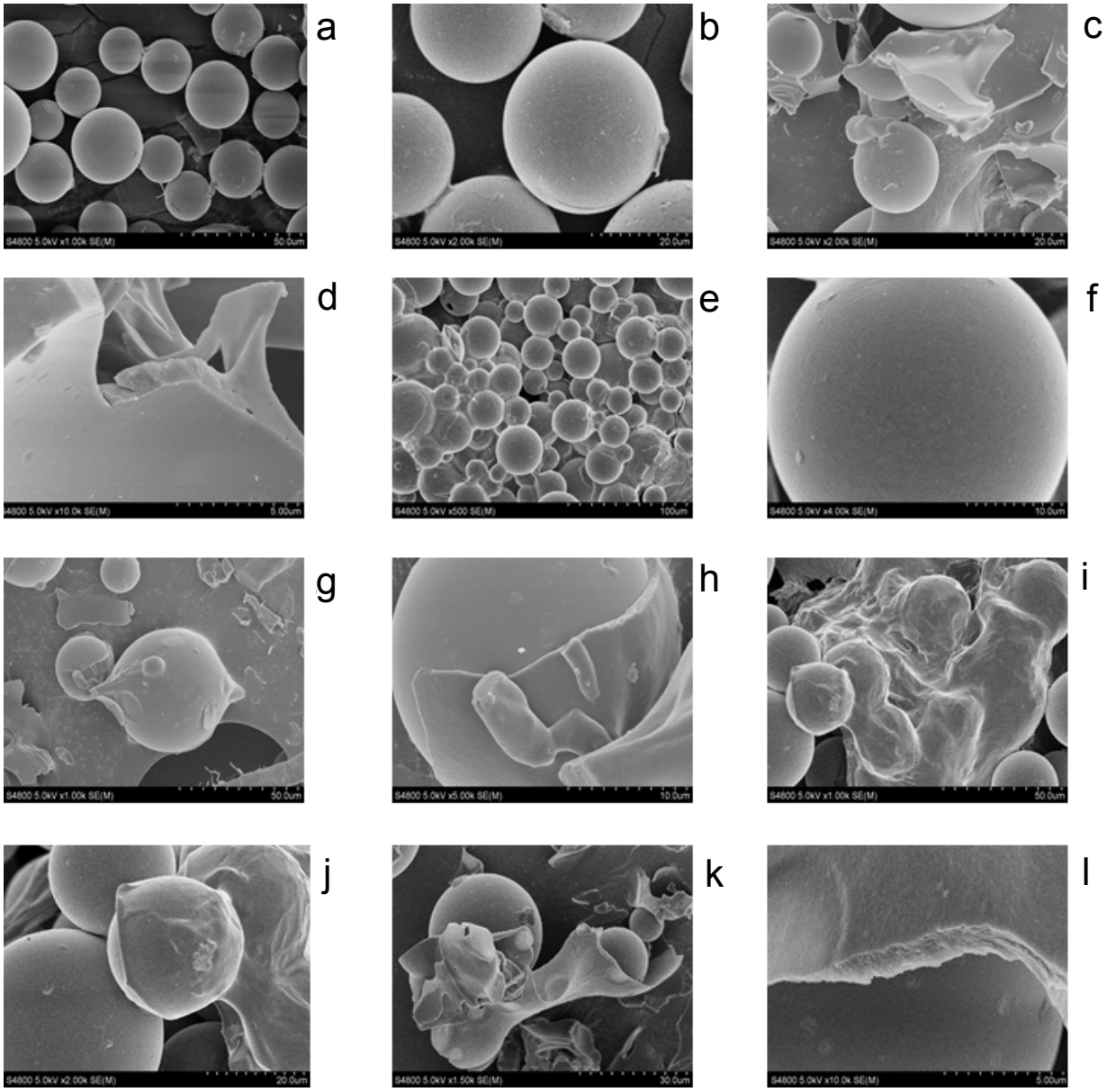

Fig. 2: Scanning electron microscopy pictures of the glass beads encapsulated with different wall materials.
(a) An overall view of G-SPP microcapsules; (b) A high magnification view of simple G-SPP microcapsule; (c) Coating of G-SPP microcapsules separated from the glass beads; (d) A high magnification view of G-SPP coating. (e) An overall view of G-GA microcapsules; (f) A high magnification view of simple G-GA microcapsule; (g) Coating of G-GA microcapsules separated from the glass beads; (h) A high magnification view of G-GA coating. (i) An overall view of G-CS microcapsules; (j) A high magnification view of simple G-CS microcapsule; (k) Coating of G-CS microcapsules separated from the glass beads; (l) A high magnification view of G-CS coating. G = gelatin; SPP = sodium polyphosphate; GA = arabic gum; CS = chitosan

occurred between core/(core+wall) ratio and pH at complex coacervation. This interaction was of a positive magnitude.

The response surface and contour plots (fig. 3) for the polynomial equation were constructed to find the optimum point at core/(core+wall) ratio of 64.12%, pH 4.31, and 3.31 mM glutaraldehyde/1 g gelatin. Three batches of microcapsules were prepared under the optimized conditions. The mean EE was 93.58% compared to the predicted value of 94.9%, with RSD of 1.38%. The result provided the adequacy of the regression models.

The SEM image of encapsulated OMC was shown in fig. 4. SEM analysis indicated that OMC microcapsules appeared spherical in shape with smooth non-porous surface and no tendency to aggregation, which was same as glass beads loaded microcapsules. The particle size distribution of OMC microcapsules was reported in fig. 5. The mean diameter of microcapsules was 3.376 μm with a RSD of 0.052, and the range was fairly narrow.

As a chemical sunscreen, the mechanism of OMC filtering the UV light is that when an OMC molecular under the ground state is inspired by an appropriate energy, electron located on the highest energy which occupied π orbit can absorb energy, and then accomplish the transition to the π* orbit, i.e., the radiation energy is converted to other

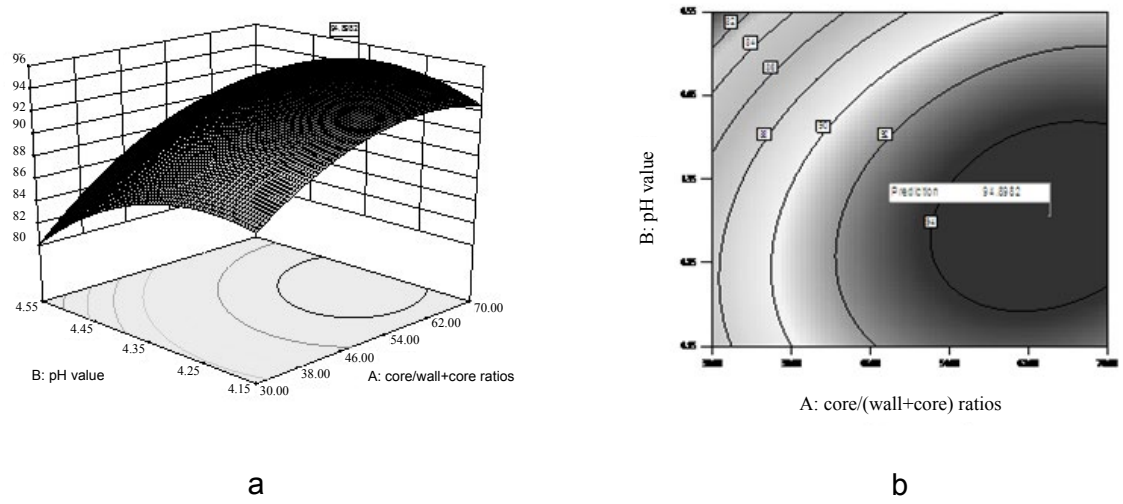

Fig. 3: Response surface and contour plots of microcapsules.
Response surface (a) and contour plots (b) of microcapsules with encapsulation efficiency of 94.9%, at 3.31 mM glutaraldehyde /1 g gelatin level.

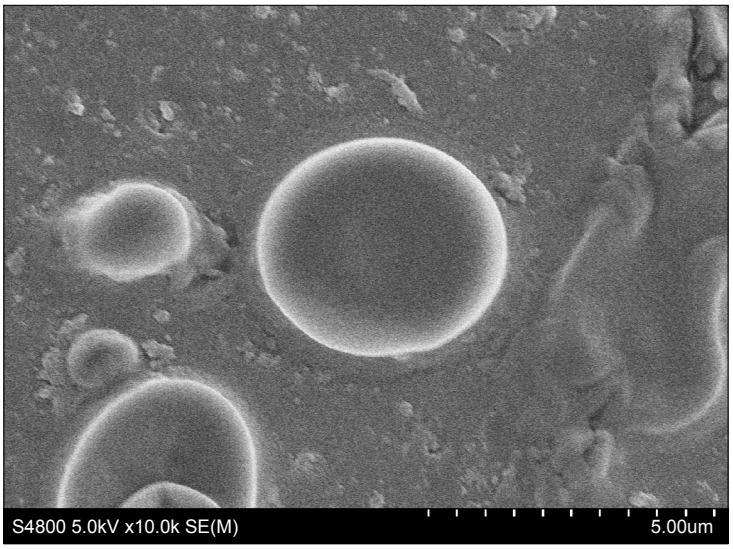

Fig. 4: Scanning electronic microscopy picture of octyl methoxycinnamate loaded microcapsules.

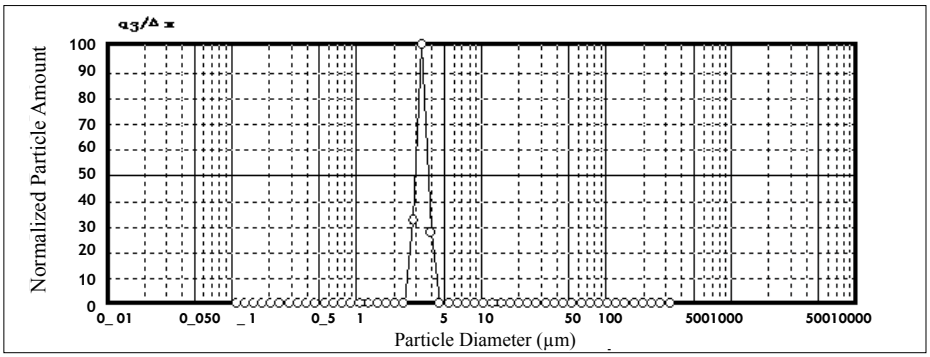

Fig. 5: Normalized particle size distribution map of octyl methoxycinnamate loaded microcapsules.

forms of energy[33,34]. In other words, more energy was absorbed, and higher percentage of OMC was photodegradated. In this work, protection from UV light was express by degradation percentage of OMC.

As shown in fig. 6, dispersion by the adsorbent (SiO_2) and microencapsulation process enhanced the photoprotection of OMC. A possible explanation for this was that surface area exposed to UV light increased by dispersion and microencapsulation. Indeed, it was indicated that high dispersity could improve photoprotective property[27]. This method was proposed to ensure an adequate efficacy of the sun blockers.

When exposing to the UV irradiation, OMC with photochemical activity occurred photochemical reactions, such as cis-trans isomerization and photodecomposition[25,35]. The degradation compound had also irritancy, allergy, and cytotoxicity, especially

in the conditions of transdermal permeation and large accumulation within the deeper layers of skin[36].

Liquid chromatogram at 280 nm for determination of photodegradation product was shown in fig. 7. The results presented in fig. 8 demonstrated the *in vitro* percutaneous absorption of OMC or its photodegradation product through porcine ear skin for the four studied formulations. As measured by OMC concentration in the receptor fluid, the extent of percutaneous absorption of the cream containing OMC microcapsules was significantly lower than that of the cream containing free OMC (4.95 µg/ml *vs.* 15.5 µg/ml at 9 h) (fig. 8a). In addition, the slow diffusion rate of OMC from the microcapsules suggested that the OMC was entirely encapsulated and not adsorbed at the external surface of the microcapsules. The concentration of photodegradation product in the receptor fluid could not be calculated in the absence of appropriate standard substance. The extent of percutaneous absorption of photodegradation product was measured quantitatively by peak area on the chromatogram. As shown in fig. 8b, the peak area was smaller for the preparation incoporating the encapsulated photodegradation product as compared to the preparation containing the free photodegradation product.

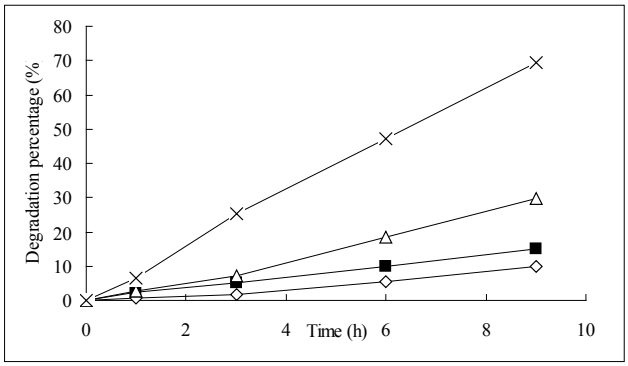

Fig. 6: The degradation percentage of OMC in the different preparations.
◇: free OMC; ■: OMC adsorbed by SiO_2; △: OMC microcapsules; ×: well-dispersed OMC microcapsules. OMC is octyl methoxycinnamate

The properties such as nontoxic and not rapidly absorbed are important considerations to examine the safety of UV filters used in sunscreens. According to the elucidation above, the cytotoxicity and skin permeation abilities of the sun filter and its photodegradation product were drastically decreased after encapsulation, which was corroborated that the sunscreens remain mainly on the outermost skin layers, shielding the skin from noxious UV radiation as effectively as possible.

The results of glass beads microencapsulation experiments suggested that the combination of gelatin and sodium polyphosphate was suitable as wall materials for entrapping OMC. An OMC-loaded microcapsule formulation was optimized using RSM by fitting a second-order model with core/(core+wall) ratio, pH at complex coacervation, and glutaraldehyde amount as independent variables, EE as dependent variable. The optimization method enabled to predict the response variable value within the experimental range with good agreement between the predicted and experimental values. The *in vitro* data demonstrated that the microencapsulation process could reduce the percutaneous absorption of OMC and its photodegradation product, and enhance the photoprotection of OMC. This study emphasized the potential of sunscreen microcapsules as new skin drug delivery systems.

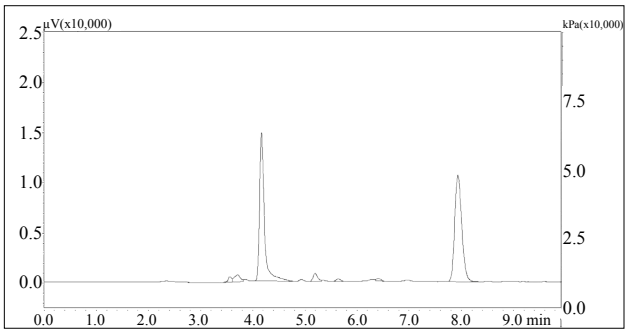

Fig. 7: Liquid chromatogram example of photodegradation product. The retention times of degradation product and OMC was 4.218 and 7.953 min, respectively. OMC is octyl methoxycinnamate

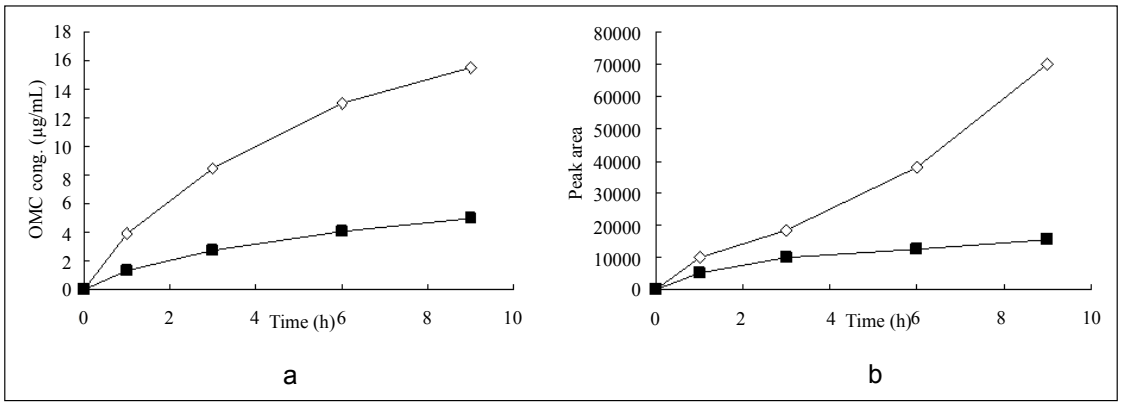

Fig. 8: The results of transdermal permeation experiments.
(a) ◇: free OMC; ■: OMC microcapsules; (b) ◇: free degradation product; ■: degradation product-loaded microcapsules. OMC is octyl methoxycinnamate

FINANCIAL ASSISTANCE

This work was supported by the grant of Educational Commission of Heilongjiang Province of China (No. 12541644).

CONFLICT OF INTERESTS

None declared.

REFERENCES

1. Dong KK, Damaghi N, Picart SD, Markova NG, Obayashi K, Okano Y, *et al.* UV-induced DNA damage initiates release of MMP-1 in human skin. Exp Dermatol 2008;17:1037-44.
2. Gallagher RP, Lee TK. Adverse effects of ultraviolet radiation: a brief review. Prog Biophys Mol Biol 2006;92:119-31.
3. Krutmann J. The interaction of UVA and UVB wavebands with particular emphasis on signalling. Prog Biophys Mol Biol 2006;92:105-7.
4. Nohynek GJ, Antignac E, Re T, Toutain H. Safety assessment of personal care products/cosmetics and their ingredients. Toxicol Appl Pharmacol 2010;243:239-59.
5. Sadrieh N, Wokovich AM, Gopee NV, Zheng J, Haines D, Parmiter D, et al. Lack of significant dermal penetration of titanium dioxide from sunscreen formulations containing nano-and submicron-size TiO_2 particles. Toxicol Sci 2010;115:156-66.
6. Touitou E, Godin B. Skin nonpenetrating sunscreens for cosmetic and pharmaceutical formulations. Clin Dermatol 2008;26:375-9.
7. Sambandan DR, Ratner D. Sunscreens: An overview and update. J Am Acad Dermatol 2011;64:748-58.
8. Kockler J, Oelgemöller M, Robertson S, Glass BD. Photostability of sunscreens. J Photochem Photobiol C Photochem Rev 2012;13:91-110.
9. Jain SK, Jain NK. Multiparticulate carriers for sun-screening agents. Int J Cosmet Sci 2010;32:89-98.
10. Klammer H, Schlecht C, Wuttke W, Schmutzler C, Gotthard I, Köhrle J, et al. Effects of a 5-day treatment with the UV-filter octyl-methoxycinnamate (OMC) on the function of the hypothalamo-pituitary-thyroid function in rats. Toxicology 2007;238:192-9.
11. Christen V, Zucchi S, Fent K. Effects of the UV-filter 2-ethyl-hexyl-4-trimethoxycinnamate (EHMC) on expression of genes involved in hormonal pathways in fathead minnows (Pimephales promelas) and link to vitellogenin induction and histology. Aquat Toxicol 2011;102:167-76.
12. Axelstad M, Boberg J, Hougaard KS, Christiansen S, Jacobsen PR, Mandrup KR, et al. Effects of pre- and postnatal exposure to the UV-filter octyl methoxycinnamate (OMC) on the reproductive, auditory and neurological development of rat offspring. Toxicol Appl Pharmacol 2011;250:278-90.
13. Klammer H, Schlecht C, Wuttke W, Jarry H. Multi-organic risk assessment of estrogenic properties of octyl-methoxycinnamate *in vivo* A 5-day sub-acute pharmacodynamic study with ovariectomized rats. Toxicology 2005;215:90-6.
14. Morohoshi K, Yamamoto H, Kamata R, Shiraishi F, Koda T, Morita M. Estrogenic activity of 37 components of commercial sunscreen lotions evaluated by *in vitro* assays. Toxicol *In Vitro* 2005;19:457-69.
15. Karlsson I, Hillerström L, Stenfeldt AL, Mårtensson J, Börje A. Photodegradation of Dibenzoylmethanes: Potential Cause of Photocontact Allergy to Sunscreens. Chem Res Toxicol 2009;22:1881-92.
16. Chatterjee S, Salaün F, Campagne C, Vaupre S, Beirão A. Preparation of microcapsules with multi-layers structure stabilized by chitosan and sodium dodecyl sulfate. Carbohydr Polym 2012;90:967-75.
17. Ocak B. Complex coacervation of collagen hydrolysate extracted from leather solid wastes and chitosan for controlled release of lavender oil. J Environ Manage 2012;100:22-8.
18. Dong Z, Ma Y, Hayat K, Jia C, Xia S, Zhang X. Morphology and release profile of microcapsules encapsulating peppermint oil by complex coacervation. J Food Eng 2011;104:455-60.
19. Neubauer MP, Poehlmann M, Fery A. Microcapsule mechanics: From stability to function. Adv Colloid Interfac 2014;207:65-80.
20. Chang CP, Leung TK, Lin SM, Hsu CC. Release properties on gelatin-gum arabic microcapsules containing camphor oil with added polystyrene. Colloid Surface B 2006;50:136-40.
21. Fang Z, Bhandari B. Encapsulation of polyphenols - a review. Trends Food Sci Tech 2010;21:510-23.
22. Lee YK, Ahn SI, Kwak HS. Optimizing microencapsulation of peanut sprout extract by response surface methodology. Food Hydrocolloid 2013;30:307-14.
23. Qv XY, Zeng ZP, Jiang JG. Preparation of lutein microencapsulation by complex coacervation method and its physicochemical properties and stability. Food Hydrocolloid 2011;25:1596-603.
24. Kage H, Kawahara H, Hamada N, Kotake T, Oe N, Ogura H. Effects of core material, operating temperature and time on microencapsulation by in situ polymerization method. Advanced Powder Technol 2002;13:377-94.
25. MacManus-Spencer LA, Tse ML, Klein JL, Kracunas AE. Aqueous photolysis of the organic ultraviolet filter chemical octyl methoxycinnamate. Environ Sci Technol 2011;45:3931-7.
26. Cilurzo F, Minghetti P, Sinico C. Newborn pig skin as model membrane in *in vitro* drug permeation studies: a technical note. AAPS PharmSciTech 2007;8:E94.
27. Wu PS, Huang LN, Guo YC, Lin CC. Effects of the novel poly(methyl methacrylate) (PMMA)-encapsulated organic ultraviolet (UV) filters on the UV absorbance and *in vitro* sun protection factor (SPF). J Photochem Photobiol B 2014;131:24-30.
28. Abreu FOMS, Oliveira EF, Paula HCB, de Paula RCM. Chitosan/cashew gum nanogels for essential oil encapsulation. Carbohyd Polym 2012;89:1277-82.
29. Brown EN, Davis AK, Jonnalagadda KD, Sottos NR. Effect of surface treatment on the hydrolytic stability of E-glass fiber bundle tensile strength. Compos Sci Technol 2005;65:129-36.
30. Dai R, Wu G, Li W, Zhou Q, Li X, Chen H. Gelatin/carboxymethylcellulose/dioctyl sulfosuccinate sodium microcapsule by complex coacervation and its application for electrophoretic display. Colloid Surface A 2010;362:84-9.
31. Woranuch S, Yoksan R. Eugenol-loaded chitosan nanoparticles: I. Thermal stability improvement of eugenol through encapsulation. Carbohyd Polym 2013;96:578-85.

32. Yuen CWM, Yip J, Liu L, Cheuk K, Kan CW, Cheung HC, et al. Chitosan microcapsules loaded with either miconazole nitrate or clotrimazole, prepared via emulsion technique. Carbohyd Polym 2012;89:795-801.
33. Alves LF, Gargano R, Alcanfor SKB, Romeiro LAS, Martins JBL. A chromophoric study of 2-ethylhexyl p-methoxycinnamate. Chem Phy Lett 2011;516:162-5.
34. Díaz-Cruz MS, Llorca M, Barcelo D. Organic UV filters and their photodegradates, metabolites and disinfection by-products in the aquatic environment. Trac-trend Anal Chem 2008;27:873-87.
35. Santos AJ, Miranda MS, Esteves da Silva JC. The degradation products of UV filters in aqueous and chlorinated aqueous solutions. Water Res 2012;46:3167-76.
36. Butt ST, Christensen T. Toxicity and phototoxicity of chemical sun filters. Radiat Prot Dosim 2000;91:283-6.

Accepted 24 Mar 2016
Revised 04 Feb 2016
Received 06 Mar 2015
Indian J Pharm Sci 2016;78(2):193-202